



SCUOLA INTERNAZIONALE SUPERIORE DI STUDI AVANZATI

SISSA Digital Library

Efficient reduction in shape parameter space dimension for ship propeller blade design

Original

Efficient reduction in shape parameter space dimension for ship propeller blade design / Mola, Andrea; Tezzele, Marco; Gadalla, Mahmoud; Valdenazzi, Federica; Grassi, Davide; Padovan, Roberta; Rozza, Gianluigi. - (2019), pp. 201-212. (Intervento presentato al convegno MARINE 2019 - VIII International Conference on Computational Methods in Marine Engineering tenutosi a Gothenburg, Sweden nel 13 May 2019-15 May 2019).

Availability:

This version is available at: 20.500.11767/90949 since: 2019-05-29T18:13:31Z

Publisher:

International Center for Numerical Methods in Engineering (CIMNE)

Published

DOI:

Terms of use:

Testo definito dall'ateneo relativo alle clausole di concessione d'uso

Publisher copyright

note finali coverpage

(Article begins on next page)

Efficient Reduction in Shape Parameter Space Dimension for Ship Propeller Blade Design

Andrea Mola^{*1}, Marco Tezzele^{†1}, Mahmoud Gadalla^{‡1},
Federica Valdenazzi^{§2}, Davide Grassi^{¶2}, Roberta Padovan^{||3}, and
Gianluigi Rozza^{**1}

¹Mathematics Area, mathLab, SISSA, International School of
Advanced Studies, via Bonomea 265, I-34136 Trieste, Italy

²CETENA S.p.A., via Ippolito D'Aste 5, I-16121 Genova, Italy

³CETENA S.p.A., Branch Office Trieste Passeggio S. Andrea, 6/A -
34100 Trieste, Italy

May 24, 2019

Abstract

In this work, we present the results of a ship propeller design optimization campaign carried out in the framework of the research project PRELICA, funded by the Friuli Venezia Giulia regional government. The main idea of this work is to operate on a multidisciplinary level to identify propeller shapes that lead to reduced tip vortex-induced pressure and increased efficiency without altering the thrust. First, a specific tool for the bottom-up construction of parameterized propeller blade geometries has been developed. The algorithm proposed operates with a user defined number of arbitrary shaped or NACA airfoil sections, and employs arbitrary degree NURBS to represent the chord, pitch, skew and rake distribution as a function of the blade radial coordinate. The control points of such curves have been modified to generate, in a fully automated way, a family of blade geometries depending on as many as 20 shape parameters. Such geometries have then been used to carry out potential flow simulations with the Boundary Element Method based software PROCAL. Given the high number of

*andrea.mola@sissa.it

†marco.tezzele@sissa.it

‡mgadalla@sissa.it

§federica.valdenazzi@cetena.it

¶davide.grassi@cetena.it

||roberta.padovan@cetena.it

**gianluigi.rozza@sissa.it

parameters considered, such a preliminary stage allowed for a fast evaluation of the performance of several hundreds of shapes. In addition, the data obtained from the potential flow simulation allowed for the application of a parameter space reduction methodology based on active subspaces (AS) property, which suggested that the main propeller performance indices are, at a first but rather accurate approximation, only depending on a single parameter which is a linear combination of all the original geometric ones. AS analysis has also been used to carry out a constrained optimization exploiting response surface method in the reduced parameter space, and a sensitivity analysis based on such surrogate model. The few selected shapes were finally used to set up high fidelity RANS simulations and select an optimal shape.

1 Introduction

In several fields of engineering, virtual prototyping simulations results depend on a wide range of different design parameters. When the number of such input parameters becomes too large, the problem of finding their combination resulting in the optimal solution can be easily affected by the curse of dimensionality. Depending on the computational cost of the single simulations, even with a relatively small parameter space dimension, a full optimization campaign could require months to be completed. Thus, reducing the dimension of such space is crucial to allow for quality optimization in engineering design processes.

In recent years, several interesting applications of shape parameter reduction techniques have been documented in the literature. Among them, we mention [6, 7], in which the authors apply both nonlinear extensions of the Principal Component Analysis (PCA) [16] and methods based on Artificial Neural Networks (ANN) [10] to approximate in low dimensional spaces the parametric deformation of ship hulls. A common feature of such works, is that they act in an *offline* fashion, since they solely operate on the relationship between shape parameters and hull geometry, rather than on the one between shape parameters and simulations output. This leads to the advantage that less simulations are required in the *online* optimization phase. In this work, we make instead use of an analysis based on the Active Subspaces (AS) property [4] to obtain parameter space reduction in the framework of a ship propeller shape optimization campaign. A main trait of the present analysis is that, differently from the ones described, it is carried out in the online phase of the optimization so as to construct a reduced parameter space to approximate the relationship between the simulations output and the parameters. Although this might lead to increased computational cost, the analysis has the fruitful benefit of identifying which of the original parameters bear a higher influence on the physical output. Such information can of course lead the work of design engineers. In addition, to mitigate the disadvantage of possibly high computational cost associated

to the high number of simulations required for the analysis, in this work we made use of the potential flow solver PROCAL [21], which despite its low computational cost, is able to provide accurate predictions of the fluid dynamic outputs of interest. Moreover, we also explore the use of AS for constrained optimization exploiting response surface method in the reduced parameter space, to identify propeller shapes with increased hydroacoustic performance (i.e.: reduced tip vortex-induced maximum pressure) without thrust reductions. The most promising shapes are the only ones tested with the high-fidelity RANS solver, with considerable reduction of the whole optimization campaign.

2 Blade reconstruction and morphing

A very important ingredient of the multidisciplinary propeller optimization methodology here described is represented by an efficient shape parameterization tool. In fact, as well known, optimization algorithms are mathematical tools which operate on numerical variables, identifying the input parameters combination which maximizes or minimizes the output values of a specific model or system. In such framework, optimization algorithms cannot be used to find shapes of optimal performance, unless a shape parameterization strategy is devised to associate each possible shape modification with numbers characterizing the points in the parameter space. Such numbers are the input used to feed the optimization algorithm. Thus, the main task of shape parameterization is that of creating a — possibly — one-to-one correspondence between propeller shapes and sample points in the parameter space. There are several multi-purpose parameterization methodologies available in the literature, which are designed to deform bodies of arbitrary shapes. Such algorithms, among which we mention Free Form Deformation (FFD) [13] and Radial Basis Functions (RBF), are implemented in open source software libraries and packages [1, 15, 19] which could be in principle readily downloaded and employed. Unfortunately, in their original formulation such multi-purpose deformation strategies are not suitable for a highly engineered shape as a ship propeller. Among other things, their application would in fact result in altering in an undesired way the specific airfoils selected by the engineers at each blade section for their well assessed hydrodynamic performance. Rather than tweaking FFD or RBF to account for constraints on the shape deformations generated, we decided to exploit the procedure used by the engineers for the bottom-up generation of 3D propeller geometries.

2.1 Bottom-up blade construction of parameterized propeller

A 3D propeller blade is generated (see for instance [3]) as the surface passing through a set of sectional airfoil shapes, which are originally specified in a

2D space and are successively located in the 3D space according to a set of transformations which vary along with the radial coordinate of each section. Such transformations include scaling, translations and rotations to obtain the blade with the desired radial distribution of airfoil section chord length, rake and skew displacements, and pitch angle respectively. Such standard propeller blade design procedure has been implemented in the open source python package BladeX [9]. As illustrated in Figure 1, after the coordinates of blade airfoil sections and radial distribution curves are read from external files, the airfoil sections are placed in the correct three dimensional position and the CAD surface passing through the sections is generated and exported in *iges* format.

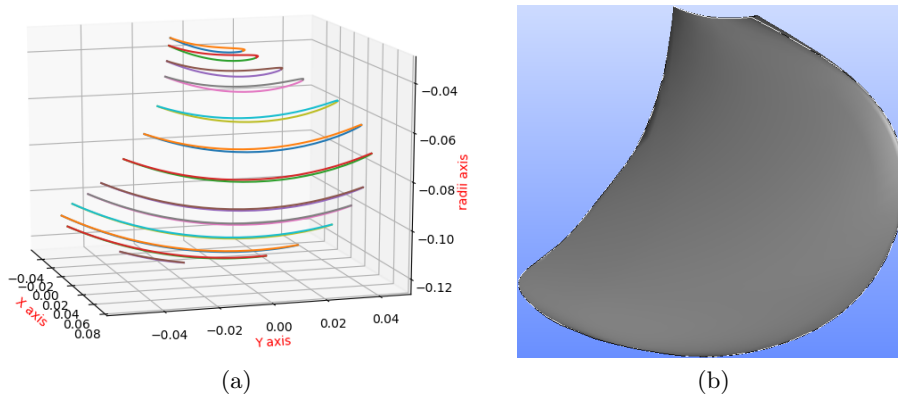


Figure 1: PPTC blade bottom-up construction with BladeX: (a) Cylindrical blade sections in their final three dimensional position. (b) The generated CAD surface (saved in *iges* file format).

In the framework of the described blade construction procedure, BladeX allows for reconstructing with user specified degree splines, the radial distribution curves for chord length, pitch angle, skew and rake displacements. By means of constrained least squares minimization, the algorithm will in fact identify the spline control points position minimizing the distance between the original curves and their splines counterparts. A further method has been added to allow for spline reconstruction of the radial distribution of the sectional airfoils maximum camber deflection. Once chord, pitch, skew, rake and camber radial distributions have been reconstructed by means of splines, the user introduces a set of splines control points displacements to alter the blade characteristic curves and ultimately its shape. Thus, a parameterized blade geometry can be generated through variations of the position of an arbitrary number of the control points associated with the spline reconstruction of the original blade characteristic curves. This obviously leads to the convenient possibility of generating parameter spaces

having the desired dimension. In addition, a further relevant advantage of such parameterization strategy based on splines control points displacement, is that all the blades generated are smooth deformations of the original one. Figure 2 shows a pitch curve reconstruction by means of a 10 control points 3rd order spline carried out through BladeX. In the example, non null displacements are also assigned to control points 6 and 7, to generate a modified pitch distribution, which would ultimately result in a different blade geometry.

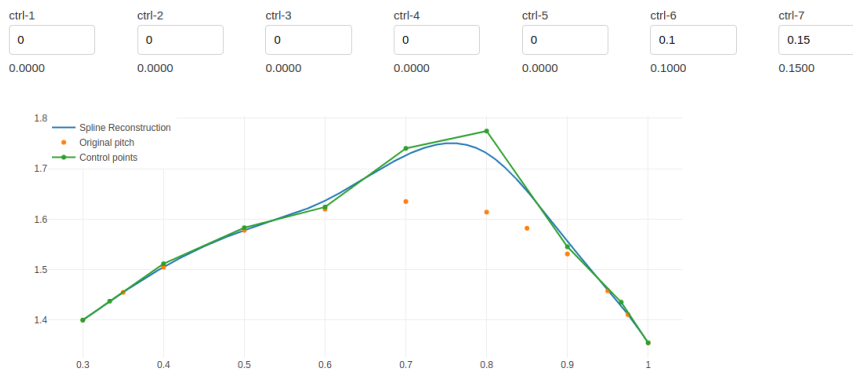


Figure 2: A sketch of the PPTC blade pitch radial distribution curve modification carried out with BladeX. The plot shows the original blade points (yellow dots), and the corresponding splines reconstruction (blue continuous line) with its control polygon (green dots and line). The example shows how control points 6 and 7 are modified to alter the pitch curve retaining smoothness.

Once the parameterized blade geometry has been generated, the full propeller geometry can be finalized by replicating the blade for the desired number of times, and attaching it to the imported hub geometry.

2.2 A family of PPTC SVA-VP1304 blade deformations for the optimization campaign

We based our analysis on the shape of the PPTC SVA-VP1304 benchmark propeller ¹, originally designed for the SMP workshops [2]. To carry out the numerical experiments, we produced a set of 1100 blade variants, based on deforming the pitch and camber radial distributions along the blade. More specifically, the deformations were obtained displacing the 10 control points of the splines reconstructing the pitch and camber profiles, within 15% and 20% of the original blade maximum local pitch and maximum local cam-

¹Geometry and documentation available at <https://www.sva-potsdam.de/en/potsdam-propeller-test-case-pptc>

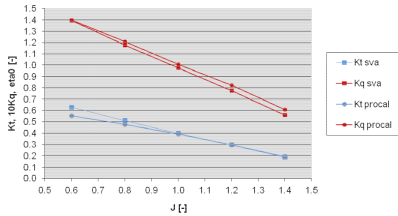
ber, respectively. We point out that the camber modification is carried out by scaling the camber line points of each sectional airfoil so as to obtain the specified local maximum camber deflection. The described methodology resulted in a family of deformations depending on 20 parameters. As the blade profiles obtained from such procedure might suffer from inflections which might lead to unfeasible manufacturing as well as the poor hydrodynamic performance, the local deformation bounds were also constrained in a way that ensures smooth profiles.

3 Parameter space analysis through active subspaces

In this section, we present the active subspaces analysis of the fluid dynamic performance results obtained for each PPTC SVA-VP1304 benchmark propeller variation produced. Such results were obtained using the potential flow solver PROCAL [21] to simulate the flow past the propeller in an open water test setup.

The present study was carried out for a single value of the propeller advance ratio $J = \frac{V_a}{n \cdot D} = 1.019$ where V_a is the streamwise velocity, $D = 0.25m$ is the propeller diameter, and n is the rotational speed in (rps). While J is a parameter summarizing the fluid dynamic inputs to the simulations, the first outputs of interest for the designers are quite naturally an estimation of the hydrodynamic forces and moments acting on the propeller. In particular, the thrust force T generated by the propeller along its axial direction is the quantity that the designers typically want to maximize. At the same time, the resisting torque Q around the propeller axis needs instead to be minimized to increase performance. Based on such considerations, the first output parameter considered in this work is the thrust coefficient $K_T = \frac{T}{\rho n^2 D^4}$ (ρ being the fluid density). As for the second output parameter, we preferred using the propeller efficiency $\eta = \frac{J}{2\pi} \cdot \frac{K_T}{K_Q}$ rather than simply using the torque coefficient $K_Q = \frac{Q}{\rho n^2 D^5}$. A high propeller efficiency is in fact a significant indicator of the propeller ability to generate thrust, without requiring high torque values from the engine to maintain the indicator of the propeller ability to generate thrust, without requiring high torque values from the engine to maintain the specific rotational speed. For the value of J herein considered, the efficiency and thrust coefficient obtained for the original PPTC SVA-VP1304 benchmark propeller are $\eta = 0.629$, $K_T = 0.3835$ respectively. As shown in Figure 3a, at the selected advance ratio the propeller thrust coefficient as predicted by a non-cavitating unsteady PROCAL computation is very close to the experimental thrust coefficient (SMP'11 workshop; test case 2.3.1 [2]), the difference amounting to less than 1%. Along with the aforementioned propeller thrust coefficient K_T and efficiency η , the output parameters also considered in the analysis were the vortex-induced maxi-

imum pressure (P_{max}), and the frequency (f_{max}) associated to (P_{max}). A summary of the values of the four outputs for the benchmark propeller are presented in Figure 3b.



Objective	Description	Value	Unit
K_T	thrust coefficient	0.3835	[-]
η	efficiency	0.629	[-]
P_{max}	max pressure induced from the tip vortices	162.3	[dB]
f_{max}	frequency at which max pressure occurs	279.9	[Hz]

(a)

(b)

Figure 3: (a) PROCAL prediction of the thrust and torque coefficients of the PPTC SVA-VP1304 at various advance ratios. Results are compared with the corresponding experimental data from the SMP workshop. (b) Computed output parameters at $J = 1.019$.

The procedure adopted in the present study is composed as follows: (i) dimension reduction via the active subspaces analysis on the geometrical parameter space defined by the the control points deformations, (ii) sensitivity analysis and optimization of the propeller performance based on the reduced parameter obtained from the active subspaces analysis. In the following subsections, we first provide a brief description of the active subspaces property theory, and then report the results of the analysis carried out on the potential flow results database.

3.1 Background and formulations

The active subspaces (AS) property has been recently establishing as one of the emerging techniques for dimension reduction in parametric studies [4, 5]. Since its introduction, AS has been widely applied in several research topics, including marine engineering [20, 18, 8], and cardio-vascular flows [17]. A parameter study of an objective function $f(\boldsymbol{\mu})$ becomes challenging when the dimension of $\boldsymbol{\mu}$ (i.e.: the number of input parameters considered) is relatively large. In that regard AS offer a sophisticated approach to reduce the study's dimensions by seeking a set of important directions in the parameter space along which f varies the most. Such directions are linear combinations of all the parameters, and span a lower dimensional subspace of the input space, which can be also exploited to carry out optimization campaigns in an extremely inexpensive fashion.

Consider the objective $f(\boldsymbol{\mu}) : \mathbb{D} \subset \mathbb{R}^m \rightarrow \mathbb{R}$ as a differentiable, square-integrable scalar function of the normalized inputs. In order to determine the directions of maximum variability we evaluate the uncentered covari-

ance matrix of gradients $\mathbf{C} = \mathbb{E}[(\nabla_{\boldsymbol{\mu}} f)(\nabla_{\boldsymbol{\mu}} f)^T] = \int_{\mathbb{D}} (\nabla_{\boldsymbol{\mu}} f)(\nabla_{\boldsymbol{\mu}} f)^T \rho d\boldsymbol{\mu}$, where $\mathbb{E}[\cdot]$ is the expectation operator, and $\rho : \mathbb{D} \rightarrow \mathbb{R}^+$ is the probability density function. The symmetric positive definite (SPD) structure of \mathbf{C} allows for an eigendecomposition, $\mathbf{C} = \mathbf{W}\boldsymbol{\Lambda}\mathbf{W}^T$, where \mathbf{W} is the $m \times m$ column matrix of eigenvectors, and $\boldsymbol{\Lambda}$ is the diagonal matrix of non-negative eigenvalues arranged in descending order. Now by partitioning $\boldsymbol{\Lambda} = \begin{bmatrix} \Lambda_1 & \\ & \Lambda_2 \end{bmatrix}$ into the larger eigenvalues, $\Lambda_1 = \text{diag}\{\lambda_1, \dots, \lambda_M\}$, and the smaller ones, $\Lambda_2 = \text{diag}\{\lambda_{M+1}, \dots, \lambda_m\}$, subsequently $\mathbf{W} = [\mathbf{W}_1 \quad \mathbf{W}_2]$ such that $\mathbf{W}_1 \in \mathbb{R}^{m \times M}$, $\mathbf{W}_2 \in \mathbb{R}^{m \times m-M}$, then the low eigenvalues Λ_2 suggest that the corresponding vectors \mathbf{W}_2 are in the null space of the covariance matrix \mathbf{C} , and such vectors can be discarded to form an approximation. Therefore the lower dimensional parameter subspace spanned by \mathbf{W}_1 is considered as the active subspace, while the inactive subspace is spanned by \mathbf{W}_2 . At this stage, the dimension reduction is achieved by projecting $\boldsymbol{\mu}$ onto the active subspace to obtain the active variables $\boldsymbol{\mu}_M = \mathbf{W}_1^T \boldsymbol{\mu} \in \mathbb{R}^M$, whereas the inactive variables are $\boldsymbol{\zeta} = \mathbf{W}_2^T \boldsymbol{\mu} \in \mathbb{R}^{m-M}$. The relationship between the full parameter space $\boldsymbol{\mu} \in \mathbb{D}$ and the active variables $\boldsymbol{\mu}_M$ is described as $\boldsymbol{\mu} = \mathbf{W}_1 \mathbf{W}_1^T \boldsymbol{\mu} + \mathbf{W}_2 \mathbf{W}_2^T \boldsymbol{\mu} = \mathbf{W}_1 \boldsymbol{\mu}_M + \mathbf{W}_2 \boldsymbol{\zeta}$, and the objective function $f(\boldsymbol{\mu})$ is approximated by $g(\boldsymbol{\mu}_M)$ which can be further exploited to construct a response surface.

3.2 Sensitivity analysis and optimization using active subspaces

According to the AS formulation presented, we consider the geometrical parameters $\boldsymbol{\mu} \in \mathbb{R}^{1100 \times 20}$ which represent the displacements of the 20 control points of all the 1100 shapes. As for the parameters ordering in vector $\boldsymbol{\mu}$, the first 10 parameters represent the pitch spline control point displacements, going from the blade root to the tip. The last 10 parameters are the camber line spline control point displacements, again ordered from root to tip. The objective function is $f_i(\boldsymbol{\mu}) \in \mathbb{R}^{1100}$, where the index $i = 1, \dots, 4$ indicates the specific output parameter considered, in the order K_T , η , P_{max} , or f_{max} . The eigendecomposition was performed on the covariance matrices corresponding to each output parameter and the resulting eigenvalues magnitudes are presented in Figure 4. The plots clearly show that for all the output parameter considered, a significant gap exists between the magnitude of first eigenvalue and that of the remaining eigenvalues. This observation suggests that each of the the input to output relationships can be rather accurately represented with a one dimensional approximation. Such one dimensional relationship is computed as the projection of the parameter space $\boldsymbol{\mu}$ onto the active subspace corresponding to the first eigenvalue (i.e.: the first eigenvector), namely $\boldsymbol{\mu}_M = \boldsymbol{\mu} \cdot \mathbf{W}_1 \in \mathbb{R}^{1100}$. In Figure 5 we show present an attempt to visualize the subspace $\mathbf{W}_1 \in \mathbb{R}^{20}$. The 20 components in each plots represent in fact the weights needed to obtain the active variable as a

linear combination of the of the original input parameters. So, such visualization is able to indicate which parameters have a higher influence on the output, as the corresponding components will be characterized by higher weight magnitudes. The results suggest that both K_T and η are mostly sensitive to the mid-to-near-tip region of the pitch profile, whereas the P_{max} and f_{max} are mostly sensitive to the near-tip region of the pitch curve. In fact, the resulting sensitivity analysis coincides with the hydrodynamic experience and the design practice, where the pitch is directly related to the loading on the propeller and to the tip vortex strength. In addition, the efficiency is directly proportional to the thrust by definition, and the blade loading, thus the K_T , is much affected by the pitch at the radial coordinate range around $0.7r/R$. Such radial coordinate is in fact used in common propeller descriptions, to provide a meaningful reference value for pitch and loading. Moreover, the plots suggest that the pitch at the tip has the largest impact on the tip vortex pressure P_{max} and subsequently f_{max} . As for the camber modifications, they appear to have on the loading a lower but still significant impact with respect to the pitch deformations, and an even less relevant effect on the tip vortex strength. A complete summary of the parameters influence on the propeller performance is presented in Table 1.

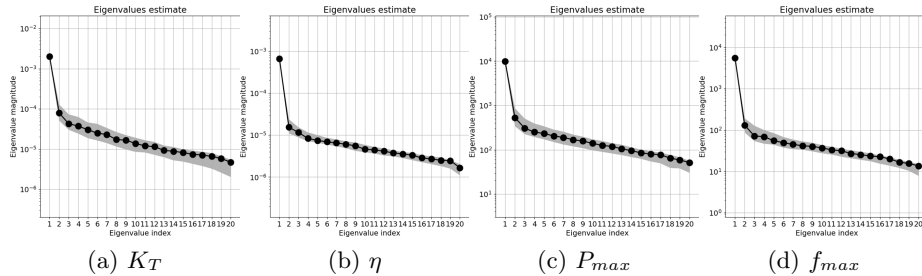


Figure 4: Eigenvalues of the uncentered covariance matrix of gradients, relating the geometrical parameters $\boldsymbol{\mu} \in \mathbb{R}^{1100 \times 20}$ to each of K_T , η , P_{max} , or f_{max} represented by $f(\boldsymbol{\mu}) \in \mathbb{R}^{1100}$. The low eigenvalues suggest the corresponding eigenvectors are in the null space of the covariance matrix, and thus a one dimensional active variable can be achieved as an approximation of $\boldsymbol{\mu}$.

We now describe a further possibility offered by AS analysis. We in fact exploit the input to output relationship in the active subspace to carry out an optimization campaign in a low dimensional —hence reduced— space. For instance, if we consider the tip vortex-induced pressure P_{max} , we can readily represent its dependence on its active variable $\boldsymbol{\mu}_M$ with a one dimensional response surface, as depicted in Figure 6a. Such response surface

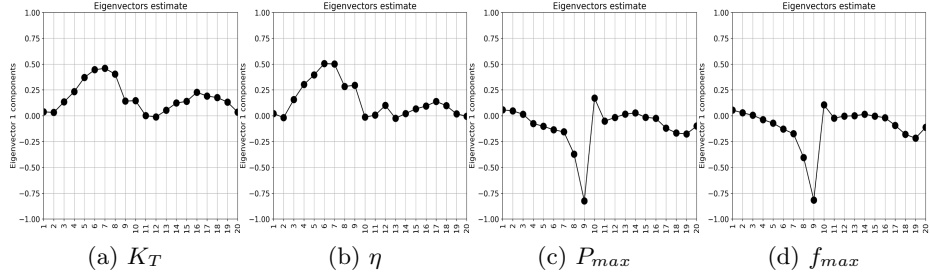


Figure 5: Components of the first eigenvector, i.e. the active subspace \mathbf{W}_1 , which describes the contribution of each of the 20 parameters in the AS approximation. The plots show that K_T and η are mostly sensitive to the mid-to-near-tip region of the pitch profile, while P_{max} and f_{max} are mostly sensitive to the near-tip region of the pitch curve.

Table 1: Summary of the PPTC performance sensitivity towards the pitch and camber root-tip parametric curves. In the table, (++) represents a dominating influence, (+): significant influence, (+-): small influence, and (-): can be neglected.

Control points	k_t	η	p_m	f_m	Control points	k_t	η	p_m	f_m
pitch - 1	-	-	+ -	+ -	camber - 1	-	-	+ -	-
pitch - 2	-	-	+ -	-	camber - 2	-	+ -	-	-
pitch - 3	+	+	-	-	camber - 3	-	-	-	-
pitch - 4	+	+	+ -	-	camber - 4	+	-	-	-
pitch - 5	++	+	+	+ -	camber - 5	+	+ -	-	-
pitch - 6	++	++	+	+	camber - 6	+	+ -	-	-
pitch - 7	++	++	+	+	camber - 7	+	+ -	+	+ -
pitch - 8	++	+	++	++	camber - 8	+	+ -	+	+
pitch - 9	+	+	++	++	camber - 9	+	-	+	+
pitch - 10	+	-	++	+	camber - 10	-	-	+	+

is then conveniently used to determine the active variable corresponding to the minimal P_{max} . The resulting optimal μ_M value is then mapped back to the actual parameter space so as to identify the exact root-tip deformations yielding the minimal acoustic pressure, as reported in Figures 6b and 7. The deformed profiles were utilized via BladeX to construct the morphed blade, Figure 6b. Finally, since the ultimate goal was to minimize P_{max} and f_{max} , maximize η without altering K_T , such procedure had to be implemented by introducing a shared subspace [11] among the four objectives, and a constrained optimization needed to be carried out on the resulting response surface in order to find the optimal propeller. Among the 1100 variants produced, the shape resulting from the procedure described was eventually

selected to undergo a high fidelity RANS simulations.

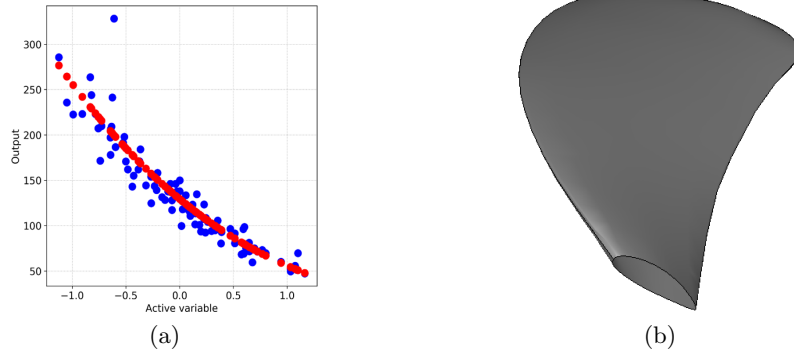


Figure 6: (a) Response surface (RS) of the reduced parameter μ_M vs. P_{max} constructed as a best-fit polynomial trained from 80% of the dataset, the remaining 20% are used to validate the output (in blue) and the corresponding RS (in red). (b) The morphed PPTC blade to produce a minimal P_{max} .

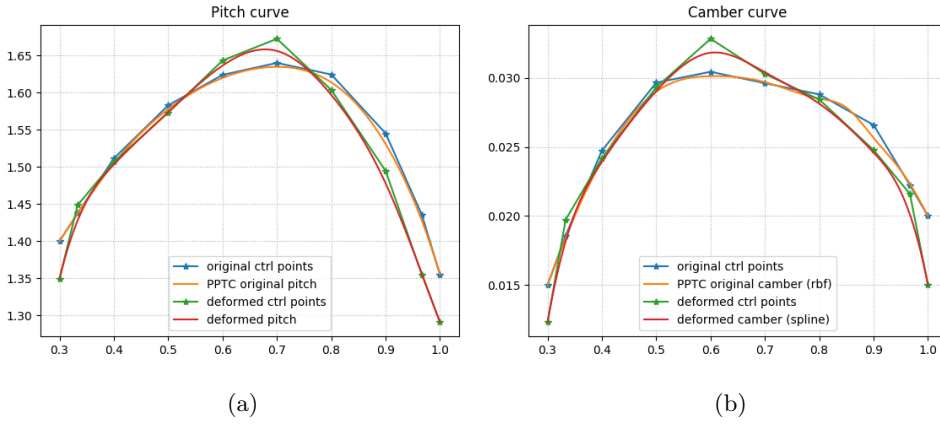


Figure 7: Deformed parametric curves resulting from the minimization procedure for P_{max} . (a) Pitch, (b) camber.

4 Conclusions and perspectives

In the present contribution, we presented an application of parameter space reduction based on the Active Subspaces (AS) property, in the framework of the hydroacoustic optimization of ship propellers. Making use of the open source Python package BladeX, we produced a large number of pa-

parameterized modifications of the PPTC SVA-VP1304 benchmark propeller, which were used to carry out potential flow simulations with the software PROCAL. The AS analysis suggested that for all the propeller performance parameters considered the input to output relationships can be rather accurately represented with a one dimensional approximation, in which the single active parameter is a linear combination of the 20 original shape parameters. A further sensitivity analysis based on the weights of such linear combination suggested that, at a first approximation, the pitch modifications in the mid-to-tip region and — at a lesser extent — the camber modification in the blade middle portion have higher impact on the output.

These results open interesting perspective on the application of parameter space reduction in naval engineering problems. Possible developments could be obtained by testing the possibility of carrying out similar investigations employing reduced fluid dynamic models, as the ones broadly described in [12] and [14]. In particular, the use of reduced order models based on POD would allow for fluid dynamic simulations that account for all the relevant physical phenomena in the flow, at a computational cost compatible with the present analysis. Ongoing work in the PRELICA project is directed in such direction.

Acknowledgements

This work was partially performed in the context of the PRELICA - “Advanced methodologies for hydro-acoustic design of naval propulsion”, supported by Regione FVG, POR-FESR 2014-2020, Piano Operativo Regionale Fondo Europeo per lo Sviluppo Regionale, and partially supported by European Union Funding for Research and Innovation — Horizon 2020 Program — in the framework of European Research Council Executive Agency: H2020 ERC CoG 2015 AROMA-CFD project 681447 “Advanced Reduced Order Methods with Applications in Computational Fluid Dynamics” P.I. Gianluigi Rozza.

References

- [1] PyGeM: Python Geometrical Morphing. Available at: <https://github.com/mathLab/PyGeM>.
- [2] U. H. Barkmann. Potsdam propeller test case (pptc) - open water tests with the model propeller vp1304, report 3752. Technical report, Schiffbau - Versuchsanstalt Potsdam, 2011.
- [3] J. Carlton. *Marine propellers and propulsion*. Butterworth-Heinemann, 1994.

- [4] P. G. Constantine. *Active subspaces: Emerging ideas for dimension reduction in parameter studies*, volume 2. SIAM, 2015.
- [5] P. G. Constantine, E. Dow, and Q. Wang. Active subspace methods in theory and practice: applications to kriging surfaces. *SIAM Journal on Scientific Computing*, 36(4):A1500–A1524, 2014.
- [6] D. D’Agostino, A. Serani, E. F. Campana, and M. Diez. Nonlinear methods for design-space dimensionality reduction in shape optimization. In *International Workshop on Machine Learning, Optimization, and Big Data*, pages 121–132. Springer, 2017.
- [7] D. D’Agostino, A. Serani, E. F. Campana, and M. Diez. Deep auto-encoder for off-line design-space dimensionality reduction in shape optimization. In *2018 AIAA/ASCE/AHS/ASC Structures, Structural Dynamics, and Materials Conference*, page 1648, 2018.
- [8] N. Demo, M. Tezzele, A. Mola, and G. Rozza. An efficient shape parametrisation by free-form deformation enhanced by active subspace for hull hydrodynamic ship design problems in open source environment. In *The 28th International Ocean and Polar Engineering Conference*, 2018.
- [9] M. Gadalla, M. Tezzele, A. Mola, and G. Rozza. BladeX: Python Blade Morphing. *The Journal of Open Source Software*, 4(34):1203, 2019.
- [10] G. E. Hinton and R. R. Salakhutdinov. Reducing the dimensionality of data with neural networks. *Science*, 313(5786):504–507, July 2006.
- [11] W. Ji, J. Wang, O. Zahm, Y. M. Marzouk, B. Yang, Z. Ren, and C. K. Law. Shared low-dimensional subspaces for propagating kinetic uncertainty to multiple outputs. *Combustion and Flame*, 190:146–157, 2018.
- [12] G. Rozza, M. W. Hess, G. Stabile, M. Tezzele, and F. Ballarin. Preliminaries and warming-up: Basic ideas and tools. In P. Benner, S. Grivet-Talocia, A. Quarteroni, G. Rozza, W. H. A. Schilders, and L. M. Silveira, editors, *Handbook on Model Order Reduction*, volume 1, chapter 1. De Gruyter, 2019.
- [13] G. Rozza, A. Koshakji, and A. Quarteroni. Free Form Deformation techniques applied to 3D shape optimization problems. *Communications in Applied and Industrial Mathematics*, 4(0):1–26, 2013.
- [14] G. Rozza, M. H. Malik, N. Demo, M. Tezzele, M. Girfoglio, G. Stabile, and A. Mola. Advances in Reduced Order Methods for Parametric Industrial Problems in Computational Fluid Dynamics. Glasgow, UK, 2018. ECCOMAS Proceedings.

- [15] F. Salmoiraghi, F. Ballarin, G. Corsi, A. Mola, M. Tezzele, and G. Rozza. Advances in geometrical parametrization and reduced order models and methods for computational fluid dynamics problems in applied sciences and engineering: Overview and perspectives. *EC-COMAS Congress 2016 - Proceedings of the 7th European Congress on Computational Methods in Applied Sciences and Engineering*, 1:1013–1031, 2016.
- [16] B. Schölkopf, A. J. Smola, and K.-R. Müller. Nonlinear component analysis as a kernel eigenvalue problem. *Neural Computation*, 10:1299–1319, 1998.
- [17] M. Tezzele, F. Ballarin, and G. Rozza. Combined parameter and model reduction of cardiovascular problems by means of active subspaces and POD-Galerkin methods. In D. Boffi, L. F. Pavarino, G. Rozza, S. Scacchi, and C. Vergara, editors, *Mathematical and Numerical Modeling of the Cardiovascular System and Applications*, pages 185–207. Springer International Publishing, 2018.
- [18] M. Tezzele, N. Demo, M. Gadalla, A. Mola, and G. Rozza. Model order reduction by means of active subspaces and dynamic mode decomposition for parametric hull shape design hydrodynamics. In *Technology and Science for the Ships of the Future: Proceedings of NAV 2018: 19th International Conference on Ship & Maritime Research*, pages 569–576. IOS Press, 2018.
- [19] M. Tezzele, N. Demo, A. Mola, and G. Rozza. An integrated data-driven computational pipeline with model order reduction for industrial and applied mathematics. *Submitted, Special Volume ECMI*, 2018.
- [20] M. Tezzele, F. Salmoiraghi, A. Mola, and G. Rozza. Dimension reduction in heterogeneous parametric spaces with application to naval engineering shape design problems. *Advanced Modeling and Simulation in Engineering Sciences*, 5(1):25, Sep 2018.
- [21] G. Vaz. *Modelling of Sheet Cavitation on Hydrofoils and Marine Propellers using Boundary Element Methods*. PhD thesis, Technical University of Lisbon -IST, 2005.